Intraoperative Navigated Angiosonography for Skull Base Tumor Surgery

Francesco Prada[1], Massimiliano Del Bene[1], Cecilia Casali[1], Andrea Saladino[1], Federico Giuseppe Legnani[1], Alessandro Perin[1], Alessandro Moiraghi[1], Carla Richetta[1], Angela Rampini[1], Luca Mattei[1], Ignazio Gaspare Vetrano[1], Riccardo Fornaro[1], Marco Saini[1], Alberto Martegani[2], Francesco DiMeco[1,3]

BACKGROUND: **One of the main challenges during skull base tumor surgery is identifying the relationships between the lesion and the principal intracranial vessels. To this end, neuronavigation systems based on preoperative imaging lack accuracy because of brain shift and brain deformation. Intraoperative navigated B-mode ultrasonography is useful in defining the extent of brain tumor. Doppler imaging adds information regarding flow entity in neighboring vessels. Second-generation ultrasound contrast agents improve the signal-to-noise ratio of B-mode imaging and permit the study of the vessel's course, blood flow, and perfusion characteristics of focal lesions. We report our experience using intraoperative navigated contrast-enhanced ultrasound to perform a navigated angiosonography (N-ASG) for the visualization of vessels in a series of 18 skull base tumors.**

METHODS: **We performed N-ASG in a series of 18 skull base tumors (10 meningiomas, 3 craniopharyngiomas, 2 giant pituitary adenomas, 1 posterior fossa epidermoid, 2 dermoid cysts). N-ASG was obtained after craniotomy before resecting each lesion and during tumor removal, after intravenous injection of ultrasound contrast agent.**

RESULTS: **In all 18 cases, major vessels and their branches were simultaneously identified (both high and low flow) using N-ASG, which allowed to visualize the whole length of each vessels. N-ASG was also useful in highlighting the lesion, compared with standard B-mode imaging, and showing its perfusion patterns.**

CONCLUSIONS: **N-ASG can be applied to skull base tumor surgery, providing helpful information about the relationship between principal intracranial vessels and tumors. This technique could be of assistance in approaching the tumor and avoiding vascular damages.**

INTRODUCTION

The skull base (SB) is an extremely complex area that includes bones, dural structures, cranial nerves, arteries, and veins. SB tumors occur relatively infrequently and represent a serious challenge for the neurosurgeon (1, 13). The surgical anatomy is highly variable and depends on the position of the tumor and contiguous SB structures.

Proper surgical planning with vessels identification is mandatory to guide the surgical strategy. Understanding vessels position in the surgical field allows for safer dissection, possibly reducing vessels injury, and permits the identification of the principal blood suppliers of the lesion, preventing severe bleeding during tumor

Key words
- Angiosonography
- Brain tumor
- Contrast-enhanced ultrasound
- Intraoperative imaging
- Intraoperative ultrasound
- Skull base surgery
- Vascular surgery

Abbreviations and Acronyms
A1: Segment A1 of anterior cerebral artery
A2: Segment A2 of anterior cerebral artery
ACA: Anterior cerebral artery
ASG: Angiosonography
CA: Contrast agent
CE: Contrast enhancement
CEUS: Contrast-enhanced ultrasound
CS: Cavernous sinus
ICA: Internal carotid artery
ioUS: Intraoperative ultrasound
MCA: Middle cerebral artery
MRI: Magnetic resonance imaging
N-ASG: Navigated angiosonography
NN: neuronavigation
SB: Skull base
TV: Temporal veins
US: Ultrasound

From the [1]Department of Neurosurgery, Fondazione IRCCS Istituto Neurologico C. Besta, Milan, Italy; [2]Department of Radiology, Ospedale Valduce, Como, Italy; and [3]Department of Neurological Surgery, Johns Hopkins Medical School, Baltimore, Maryland, USA

To whom correspondence should be addressed: Francesco Prada, M.D. [E-mail: francesco.prada@istituto-besta.it]

Supplementary digital content available online.

Citation: World Neurosurg. (2015) 84, 6:1699-1707.
http://dx.doi.org/10.1016/j.wneu.2015.07.025

Journal homepage: www.WORLDNEUROSURGERY.org

Available online: www.sciencedirect.com

removal. Therefore, vessel identification before surgical resection is highly desirable to perform a safer and more effective surgical procedure (18, 19, 22).

In this effort neuronavigation (NN), based on preoperative imaging such as computed tomography and magnetic resonance imaging (MRI), is useful to plan the surgical approach, to recognize critical structures and to direct the resection of SB tumors (18). However, NN is based on preoperative imaging that does not consider changes that occur during surgery, such as brain retraction, cerebrospinal fluid drainage, and tumor resection, all of which make the system inaccurate (10).

To overcome this limitation, an NN system coupled with intraoperative ultrasound (ioUS) has been introduced (14, 15). ioUS imaging in neurosurgery has been proved useful, especially in surgical tumor resection thanks to the real-time characteristics of the imaging, repeatability, and the possibility to differentiate between tumor and other structures (3, 6, 8, 14, 15, 21, 23). Real-time intraoperative fusion imaging between preoperative images and ioUS allows the updating of the preoperative imaging dataset, accounting for brain shift and brain deformation. As a consequence, NN coupled with ioUS could be used for the entire duration of tumor removal, relying on its indications (14, 15, 20).

Doppler imaging can be used to evaluate blood flow in arteries and veins. ioUS with color Doppler is used to visualize tumor-encased or displaced vessels and main tumor vascular suppliers. It facilitates the identification of important neurovascular structures during tumor removal, but has some limitations: angle of insonation susceptibility, low flow veins are not always visible, small vessels may be overestimated because of blooming artifacts that scatter color signals near the vessel margins (24). Furthermore, displaced vessels do not have a linear course, and it is difficult to follow them along their course with a proper insonation angle, also because of the limit imposed by the margins of craniotomy, reducing the accuracy of the Doppler signal (15). Power Doppler is less susceptible to angle of insonation, is more sensitive to flow, and is able to visualize low flow vessels, with reduced aliasing and better vessel definition (20); however, it has a poor temporal resolution, and it is difficult to follow the vessels along their course. With combined color Doppler and power Doppler, it is extremely difficult to visualize in detail and, more importantly, simultaneously arterial and venous flows, as well as tumor and organ perfusion.

A prospective tool to study the vascular anatomy and tumor perfusion with ioUS consists of using an ultrasound contrast agent (CA) to perform real-time angiosonography (ASG) (2, 4, 5, 7, 11, 16, 17). Contrast-enhanced ultrasound (CEUS) uses microbubbles (5 μm in diameter) of gas stabilized by a phospholipid shell that behave as a purely intravascular agent. The microbubbles are injected intravenously and can be transported across the lungs, allowing imaging of the arterial and venous system with a peripheral venous injection. Microbubbles hit by low-acoustic-power ultrasound (US) waves start to resonate and reflect US and thus produce US with specific harmonics (12). These harmonics are then detected and elaborated by the transducer through contrast-specific algorithms, allowing for a better identification of vascular structure, both physiological and pathological (5, 9, 11, 24).

CEUS in neurosurgery has been explored by various authors, including our group, to enhance B-mode imaging, to highlight the tumor, and to evaluate the perfusion characteristics of different cerebral lesions (2, 4, 5, 7, 11, 16, 17).

In this article, we describe the application of an intraoperative navigated angiosonography (N-ASG) technique for SB tumor surgery to define surgical planning and to identify and locate displaced or encased major vascular structures, feeding arteries, and draining veins, which will guide tumor resection and facilitate vessel identification and dissection, limiting potential injury to major vascular structures.

MATERIALS AND METHODS

Patient Population and Equipment

We evaluated patients bearing tumorlike SB masses, which were judged surgically resectable, in good general status (American Society of Anesthesiologists I–III; Karnofsky Performance Scale > 70) operated on at the Fondazione Istituto di Ricovero e Cura a Carattere Scientifico Istituto Neurologico C. Besta (Milan, Italy). Surgery was performed with the aid of fusion imaging between preoperative MRI and ioUS, allowing for navigated B-mode scan, color Doppler, and N-ASG in accordance with our institutional review board. All patients were thoroughly informed about the surgical procedure, and written consent was obtained.

Patients underwent a preoperative volumetric MRI (Siemens, Holland) with T1, T1 with gadolinium, T2-and FLAIR-weighted sequences. In all cases, surgical approach was planned using a last-generation US system (Esaote MyLab, Esaote, Italy), equipped with Fusion Imaging for NN (MedCom, Darmstadt, Germany). The US system uses the Virtual Navigator software to perform image fusion between preoperative imaging and real-time ioUS, allowing real-time NN. The navigated ioUS system displays simultaneously on the screen the real-time US imaging and the corresponding MRI generated by the three-dimensional preoperative dataset as described previously (14) (**Figure 1**).

For ioUS B-mode, Doppler, and N-ASG evaluation, we used a multifrequency (3–11 MHz) navigated linear probe (3.6 × 1 cm) (14). As a CA, we used sulfur-hexafluoride microbubbles, a second-generation US CA (SonoVue, Bracco, Italy) (16, 17).

Navigated Intraoperative B-Mode US

Before surgery (72 h), the patient underwent a preoperative volumetric MRI weighted in T1, T1 with gadolinium, T2, and FLAIR sequences that were later imported in DICOM format in the US system. The patient is positioned on the surgical table using a three-pin head-holder linked to a support for the magnetic transmitter. The registration procedure of the MRI three-dimensional dataset and the real-time US scan is then performed as described previously (14).

The site of the craniotomy is tailored on the positioned patient's head using a tracked pointer, relying on preoperative imaging. After craniotomy has been perfomed a B-mode scan (before opening the dura mater) facilitates of the registration accuracy and between tumor and other structures (**Figures 1–3**). Based on the initial registration, the US imaging and the correspondent preoperative MRI are shown on the screen of the US system and are merged together by means of overblending (**Figure 1**).

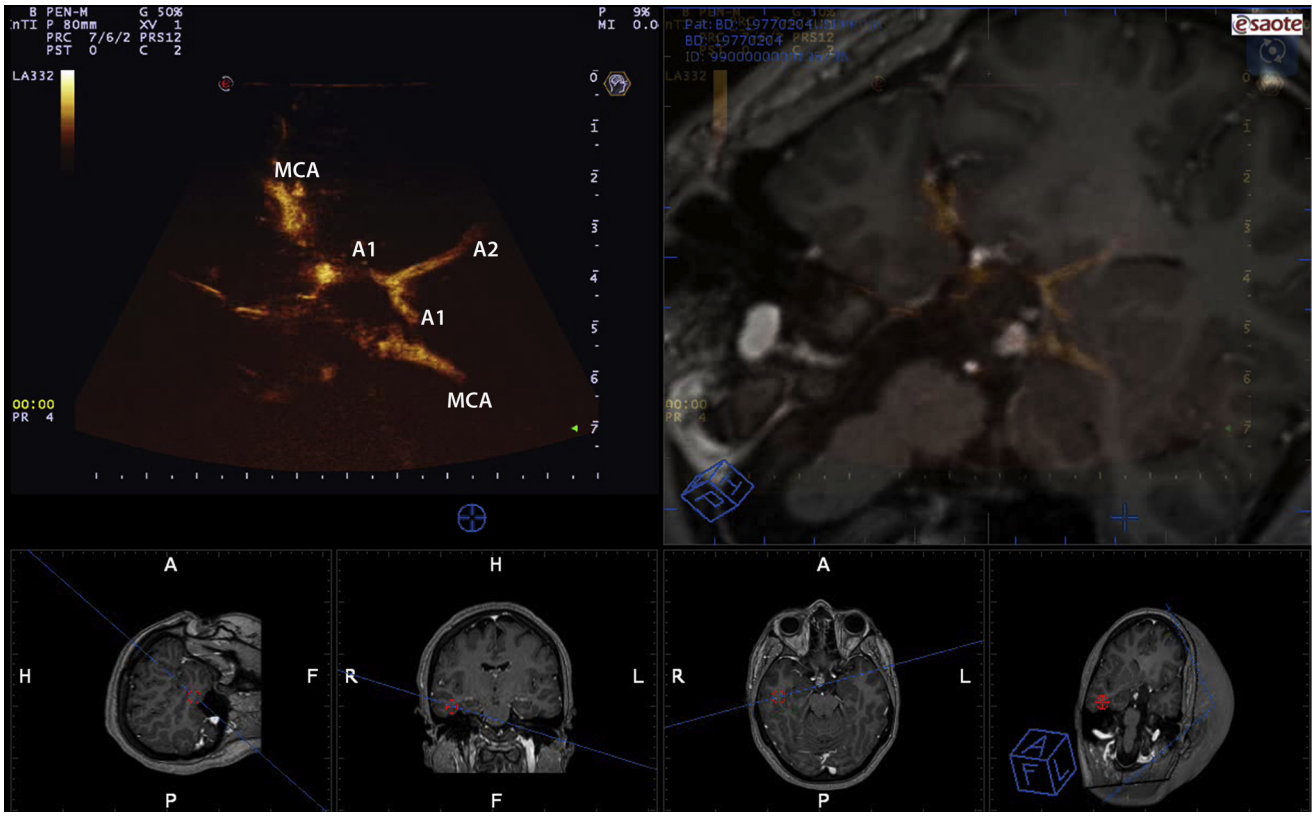

Figure 1. N-ASG screenshot of a craniopharyngioma. In the left upper portion of the screen, the ASG image is displayed. On the right side, the corresponding preoperative MRI is fused and superimposed with real-time ASG. In the lower panel, the three standard orthogonal planes (sagittal, coronal, axial) and the isonation plane are displayed. N-ASG identifies the anterior part of the polygon of Willis: the middle cerebral arteries (MCA) and the A1 and A2 segments of anterior cerebral arteries surrounding the tumor.

When a misalignment in fusion imaging occurs between the position of a structure on ioUS and the related structure on preoperative MRI, the error is corrected by fine-tuning to regain the perfect alignment (14).

At the end of tumor removal, the cavity is scanned looking for residual mass, also comparing it with the merged preoperative MRI.

Navigated Color Doppler Angiography

After lesion evaluation with navigated B-mode, color Doppler imaging is used with the in-factory vascular setup to visualize main arterial and venous trunks, and to evaluate the flow entity to correctly interpret the ASG information (**Figures 2, 3**). Traditionally, the first color Doppler scan is performed with intact dura mater together with fine-tuning; later during surgery, this analysis is repeated several times and always before N-ASG.

N-ASG

After having scanned the lesion with navigated US in B-mode and with color Doppler, N-ASG is performed as described previously (15-17); hexafluoride-filled lipidic microbubbles are injected intravenously and insonated with a linear US probe using low-power US for continuous imaging (**Figures 1–4**). The acquired harmonic signals are transduced with a CNTI algorithm, which develops a selective sensitivity of the US system to the signal produced by the microbubbles after stimulation with a single-frequency pulse at the sulfur hexafluoride resonance frequency.

Before injection, the US probe is positioned below the level of the lesion. Next, contrast agent is injected intravenously by the anesthesiologist, as a bolus of 2.4 mL (5 mg/mL), followed by a flush of 10 ml of saline solution. Concurrently, the timer is started and video clips are registered continuously during baseline US scanning and during the different vascular phases.

A first intraoperative N-ASG qualitative analysis is performed by the two surgeons. A navigated pointer displays the position of the vessels in the three-dimensional frame. The digital clips were also retrospectively reviewed to confirm the intraoperative findings.

RESULTS

In the last two years, 18 SB tumors (10 meningiomas, 3 craniopharyngiomas, 2 giant pituitary adenomas, 1 posterior fossa epidermoid, and 2 parasellar dermoid cysts) were evaluated with N-ASG (**Table 1**).

We did not notice any adverse events or side effects related to the administration of the ultrasound contrast agent.

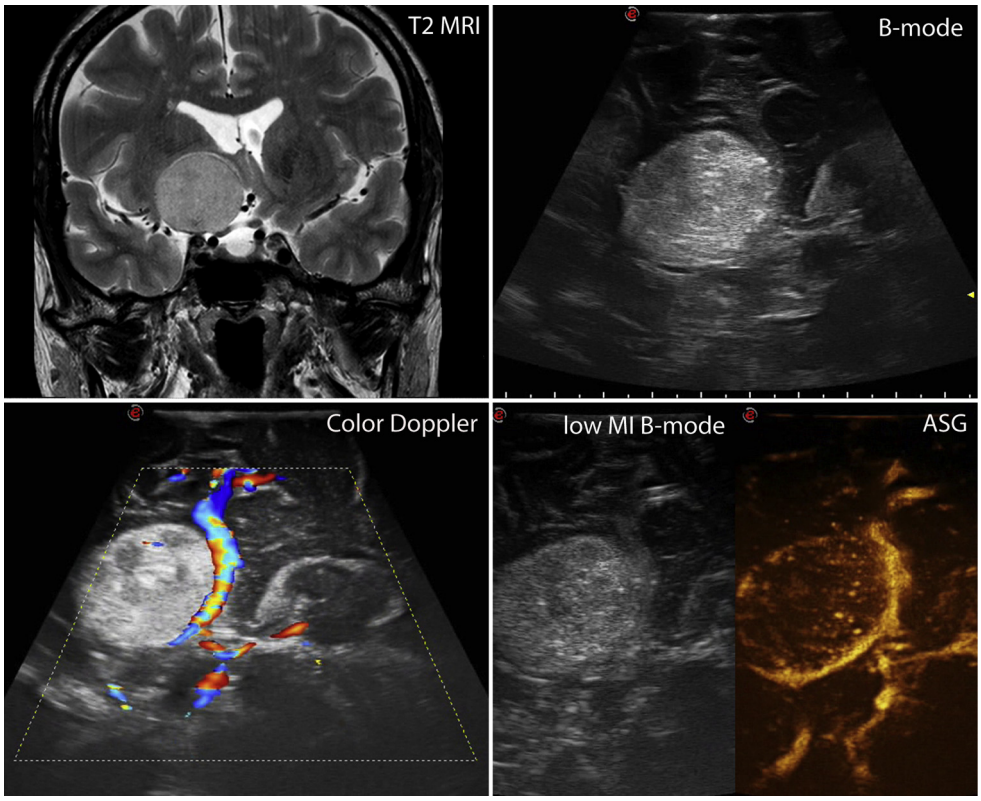

Figure 2. Multimodal appearance in a case of a right clinoid meningioma (coronal T2 WI MRI, B-mode, color Doppler, ASG). The lesion is surrounded by the middle cerebral artery (MCA) that is stretched posteriorly. In B-mode, the lesion appears hyperechoic, homogenously granular in aspect, and the calcifications are clearly visible. Color Doppler shows the right MCA, with a turbulent flow, confirming it to be a high-flow vessel. In angiosonography, tumor is identifiable together with the polygon of Willis, MCA bilaterally, and right A1 and A2.

We were able to visualize all lesions on B-mode, evaluate the major vessels with color Doppler angiography, and then further define and localize them with the N-ASG technique, with a complete interobserver agreement on both intraoperative and postoperative analyses (Table 1).

In all cases, we had a good correlation of fusion imaging between ioUS and preoperative MRI, and the correspondence between the 2 imaging modalities had a mean error of less than 2 mm. In each case, we were able to identify the lesion and major anatomic landmarks on US and to compare these findings in the coplanar MRI.

With the Doppler technique, we visualized major vessels such as internal carotid artery (ICA), middle cerebral artery (MCA), and basilar artery with few minor branches. However, it was not possible to follow the complete course of the vessels involved by the tumor or to visualize multiple vessels simultaneously (Figures 2, 3).

Ten meningiomas were located in the anterior and middle cranial fossa (3 olfactory groove, 5 clinoid, and 2 parasellar) and were all approached via a frontolateral approach. On standard US B-mode imaging, they all appeared hyperechoic with granular and sparse calcification. Maximum diameter ranged from 3 to 7 cm. All meningiomas were homogeneous and clearly demarcated from surrounding brain tissue, even in the edematous areas.

Navigated color Doppler showed the first tract of the anterior cerebral arteries (ACAs; A1) but did not show the distal branches (A2) in olfactory groove meningiomas. The ICA and MCA were not always completely visible with color Doppler in the parasellar and clinoid cases.

With N-ASG, the major vessels were identified in all cases (Figures 1–4, Video 1). In particular, in the two olfactory groove meningioma the cavernous sinus (CS), the superior sagittal sinus, the principal temporal veins (TV) and the ACA A1-A2 complex were highlighted, with the arteries displaced posteriorly. With the pure clinoid cases, the CS, TV, ICA, ACA A1 and MCA were visualized and located underneath and behind the lesion (Figures 2, 4). In three cases, the ICA was stretched and elongated with a high bifurcation, whereas in two cases the ICA was just displaced inferiorly with a low bifurcation and stretched ACA and MCA. Two parasellar meningiomas completely surrounded the ICA until the bifurcation and had close relationships with the CS (Figure 3). In all cases, small vessels (e.g., arterial perforators measuring less than 1mm) were visualized (Video 1). All meningiomas presented an intense and rapid contrast enhancement (CE; arterial phase, 5–10 seconds). The enhancement progression was centripetal with the major feeders from the dural connection. All the meningiomas had a

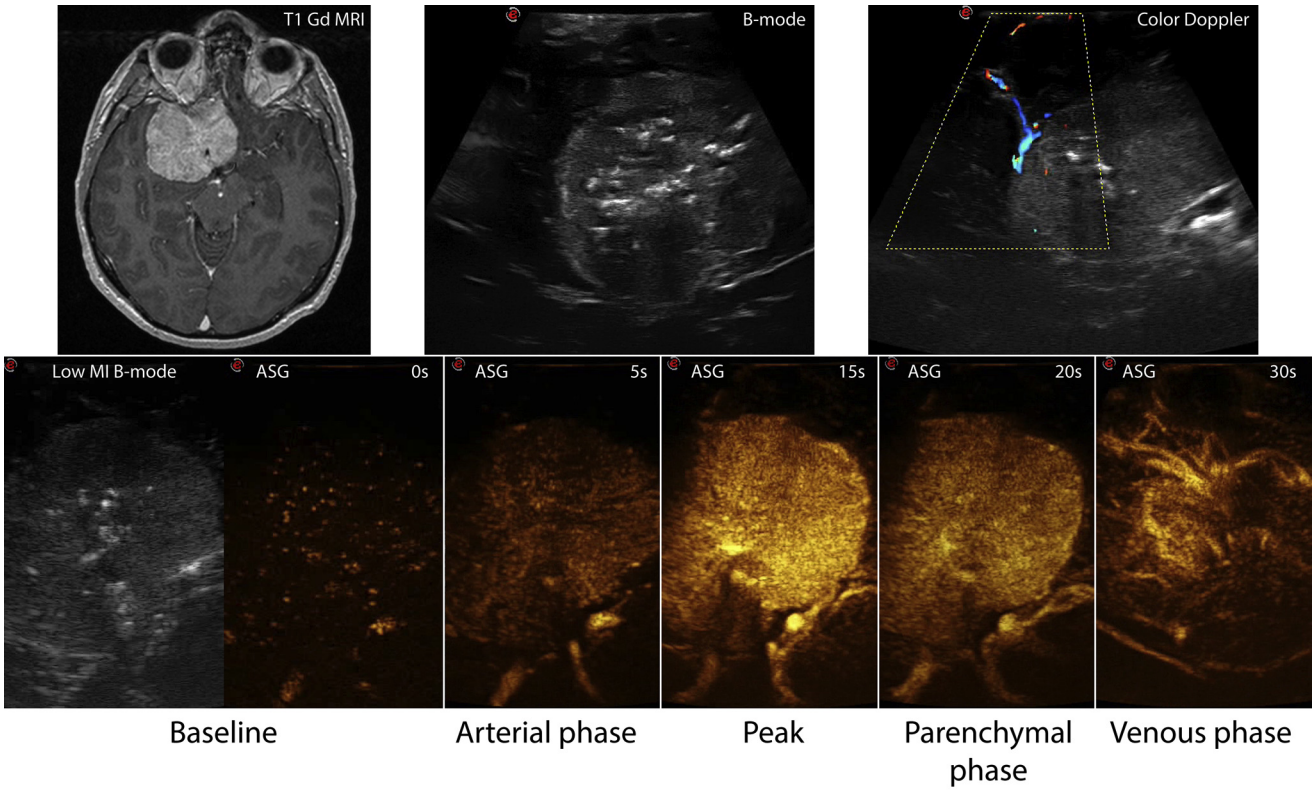

Figure 3. CEUS perfusion pattern in a case of right parasellar meningioma. The lesion encases the middle cerebral artery that is elongated posteriorly. In B-mode, the lesion appears iso-hyperechoic, with calcifications that are clearly hyperechoic. Tumor–brain interface is recognizable. Color Doppler depicts only principal vascular structure, whereas AGS simultaneously visualizes high- and low-flow vessels, allowing one to evaluate the afferent vessels and microcirculation of the tumor parenchyma. In the lower panel, the main phases of tumor perfusion are shown.

persistent parenchymal enhancement. The venous phase was delayed (30 seconds), and venous drainage was not clearly visible (**Figure 3**, **Video 1**). In all cases, the main vessels within the tumor were visible and distinguishable from the parenchymal enhancement because of tumor microcirculation. Tumor boundaries were appreciable in every case.

Three craniopharyngiomas were purely suprasellar, both with cystic components. One lesion appeared with a large perinodular cyst. The maximum diameter was 4 cm. They had a heterogeneous aspect on B-mode imaging (hyperechoic with hypoechoic cystic areas). They had a multilobular appearance with clearly demarcated boundaries. In craniopharyngiomas, color Doppler depicted major surrounding vessels, but not in a simultaneous fashion, and vascularized areas neighboring cystic areas. After CA injection, the polygon of Willis was clearly visible together with CS, also with different projections (**Figure 1**). Craniopharyngiomas had a slow arterial phase (40–50 seconds) and a delayed CE peak (80 seconds after CA arrival). The enhancement pattern was heterogeneous, and feeding and draining vessels were not visible. No vessels were recognizable inside the lesion. The parenchymal phase was persistent with a slow venous phase (100 seconds).

Video

Video available at WORLDNEUROSURGERY.org

Two large sellar/suprasellar pituitary adenomas were approached transcranially via a pterional approach. They were homogeneously hyperechoic and had a discrete multilobular appearance with clearly demarcated borders. Maximum diameter was 5 cm. With N-ASG, the polygon of Willis surrounding both lesions and the cavernous sinus were clearly highlighted. The pituitary adenomas had a relative slow arterial phase (10 seconds) and a delayed CE peak (30 seconds after CA arrival). Arterial supply was not visible, as well as the venous drainage and the CE pattern was quite regular and homogeneous. No vessels were visible. Parenchymal phase was persistent with a slow venous phase (>40 seconds after CA arrival).

One posterior cerebellar angle epidermoid cyst appeared completely hypoechoic with multiple septi on B-mode imaging, and cranial nerves V, VII, and VIII were lying within the lesion. The maximum diameter was 7 cm. Two parasellar dermoid cases (maximum diameter, 6 cm) were mainly hypoechoic with hyperechoic areas because of the presence of fatty tissue and calcifications. In all cases, the dermoid cysts were well demarcated from surrounding structures. Doppler imaging partially showed main vessels, such as MCA, but a proper vascular tree within the lesion was not appreciable. In all cases, N-ASG simultaneously

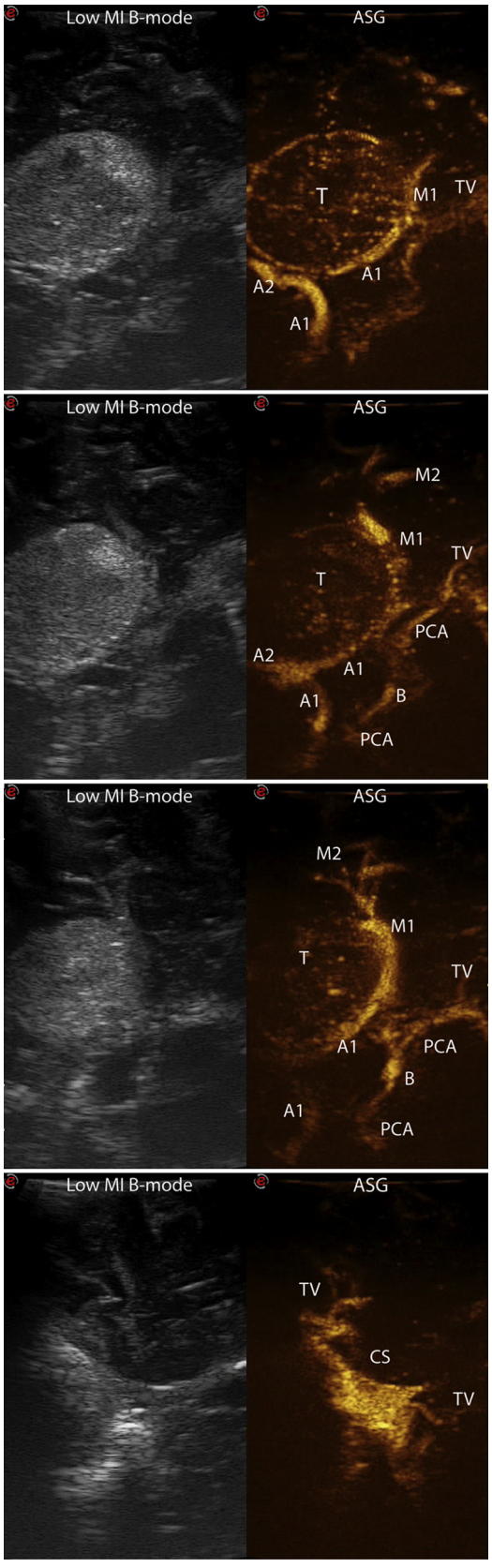

showed the major vessels with different insonation angles: the sigmoid sinus, the inferior petrosal sinus, the vertebral artery, and basilar artery near the epidermoid lesion; and the CS, the TV, and the ICA, ACA, MCA complex in the two parasellar dermoid lesions, as well as posterior circulation. Neither dermoid nor epidermoid lesions showed any appreciable contrast enhancement with N-ASG.

DISCUSSION

N-ASG facilitated the identification of the main vessels and their branches engulfed or dislocated by the lesion in all studied SB lesions (**Figures 1–4**, **Table 1**). We were able to study all the vessels included in the ioUS tomographic section, following the course of the vascular tree simply by tilting the probe, with an excellent spatial and temporal resolution.

Indeed, N-ASG provided a sufficient signal-to-noise ratio for the simultaneous visualization of major arteries and veins and their branches encased or neighboring the lesions in all cases. Moreover, tumor-feeding arteries, draining vessels, smaller vessels distributed within and around the tumor (e.g., perforators, arteries) and tumor perfusion were highlighted with N-ASG (**Video 1**). Furthermore, it was possible to perform a direct qualitative analysis of flow direction and entity simply by observing the direction of the microbubbles and the intensity of the signal.

As described previously (14), navigated B-mode US is helpful in correcting brain shift and tissue distortion, and it allows for true real-time feedback during surgery, permitting a better understanding of ioUS images.

The navigation system, coupled with contrast-enhanced ioUS with preoperative MRI (N-ASG), allowed for an easier understanding of the orientation and disposition of the vessels in the three-dimensional frame; it facilitates spatial localization of vessels within the surgical field. This feature is especially useful with approaches such as the frontolateral and the retrosigmoid, which are not fully encoded from an echographic point of view, facilitating the task to localize and preserve the vessels during dissection or leaving a residue. Fusion imaging of ASG and preoperative MRI allowed us to identify and localize major vessels within the surgical field in all cases.

It is a common belief that SB surgery is not an easy undertaking for several reasons. First, it is important to minimize the risk of injuries to vital vessels or sinuses. SB tumors frequently involve normal vascular structures or adhere to them (1, 13, 18, 19, 22). During tumor resection, it is crucial to recognize critical structures promptly to dissect the tumor. Another problem regards those lesions harboring an important vascularization and a vascular peduncle. In those tumors, like meningiomas, it is mandatory to identify and sacrifice the principal feeders rapidly to reduce the

Figure 4. Angiosonography (ASG) sequence of a right clinoid meningioma. The sequence depicts how, by tilting the ultrasound probe while performing ASG, it is possible to follow the entire course of a vessel of interest and to study all the vascular structures (e.g., arteries, microcirculation, veins) near the lesion. A1, Segment A1 of anterior cerebral artery; A2, segment A2 of anterior cerebral artery; B, tip of basilar artery; CS, cavernous sinus; ICA: internal carotid artery; M1, segment M1 of middle cerebral artery; M2, segment M2 of middle cerebral artery; PCA, posterior cerebral artery; T, tumor; TV, temporal veins.

Table 1. Result Summary

Patient No.	Diagnosis	Location	Dimensions (mm)	B-mode	Angiosonography					
					Observed Arteries	Observed Veins	Afferent Vessels	Efferent Vessels	CE Pattern	Perilesional Vessels Identification
1	Meningioma	Olfactory Groove	30 × 46	Hyperechoic, with granular and sparse calcification; homogeneous and clearly demarcated from surrounding brain tissue	ACA: A1-A2	CS, SSS, TV	Visible	Visible	Centripetal with the major feeders from the dural connection; rapid arterial phase; persistent parenchymal enhancement; delayed venous phase	Yes
2	Meningioma	Olfactory Groove	45 × 41		ACA: A1-A2	CS, SSS, TV	Visible	Visible		Yes
3	Meningioma	Olfactory Groove	50 × 65		ACA: A1-A2	CS, SSS, TV	Visible	Visible		Yes
4	Meningioma	Anterior Clinoid	61 × 68		ICA, ACA, MCA	CS, TV	Visible	Visible		Yes
5	Meningioma	Anterior Clinoid	56 × 49		ICA, ACA, MCA	CS, TV	Visible	Visible		Yes
6	Meningioma	Anterior Clinoid	47 × 48		ICA, ACA, MCA	CS, TV	Visible	Visible		Yes
7	Meningioma	Anterior Clinoid	55 × 45		ICA, ACA, MCA	CS, TV	Visible	Visible		Yes
8	Meningioma	Anterior Clinoid	37 × 48		ICA, ACA, MCA	CS, TV	Visible	Visible		Yes
9	Meningioma	Para-Sellar	70 × 53		ICA, ACA, MCA	CS	Visible	Visible		Yes
10	Meningioma	Para-Sellar	67 × 58		ICA, ACA, MCA	CS	Visible	Visible		Yes
11	Craniopharyngioma	Sellar/Supra-Sellar	40 × 31	Hyperechoic with hypoechoic cystic areas; heterogeneous with multilobular appearance and clearly demarcated boundaries	Poligone of Willis	CS	Not visible	Not clearly visible	Diffuse, nodular, heterogeneous; slow arterial phase; persistent parenchymal enhancement; delayed venous phase	Yes
12	Craniopharyngioma	Sellar/Supra-Sellar	37 × 40		Poligone of Willis	CS	Not visible	Not clearly visible		Yes
13	Craniopharyngioma	Sellar/Supra-Sellar	35 × 39		Poligone of Willis	CS	Not visible	Not clearly visible		Yes
14	Giant Pituitary Adenoma	Sellar/Supra-Sellar	40 × 49	Hyperechoic, homogenous with a discrete multi-lobular appearance and clear demarcated borders	Poligone of Willis	CS	Not visible	Not clearly visible	Diffuse, homogeneous, centrifugal; slow arterial phase; persistent parenchymal enhancement; delayed venous phase	Yes
15	Giant Pituitary Adenoma	Sellar/Supra-Sellar	50 × 38		Poligone of Willis	CS	Not visible	Not clearly visible		Yes
16	Epidermoid Cyst	Cerebello-pontine Angle	70 × 41	Completely hypoechoic with multiple septi	VA; BA	SS, IPS	Not visible	Not clearly visible	Contrast enhancement is absent; few small vessels are visible within the cyst	Yes
17	Dermoid Cyst	Para-Sellar	60 × 55	Mainly hypoechoic with hyperechoic areas due to the presence of fatty tissue and calcifications	ICA, ACA, MCA	CS, TV	Not visible	Not clearly visible		Yes
18	Dermoid Cyst	Para-Sellar	47 × 53		ICA, ACA, MCA	CS, TV	Not visible	Not clearly visible		Yes

A1, segment A1 of anterior cerebral artery; A2, segment A2 of anterior cerebral artery; ACA, anterior cerebral artery; BA, basilar artery; CE, contrast enhancement; CS, cavernous sinus; ICA, internal carotid artery; IPS, inferior petrosal sinus; MCA, middle cerebral artery; SS, sigmoid sinus; SSS, superior sagittal sinus; TV, temporal veins; VA, vertebral artery.

bleeding entity. Finally, at the end of the surgery, it is crucial to realize whether residual tumor is still present and where it is located (8, 19, 20).

Intraoperative imaging systems such as neuronavigation and ioUS (B-mode, ioUS color Doppler, and contrast-enhanced ioUS) have been developed to overcome these problems. Each of these systems has specific limitations that make one single method insufficient for the complexity of SB surgery.

Currently, in most cases surgery is guided by preoperatively acquired images that provide a wide view of the tumor and its relationships. On the other hand, this system is significantly limited by the loss of accuracy because of brain shift and brain deformation; moreover, it is inadequate in depicting small vessels (10, 20).

ioUS B-mode as an embedded value allows the identification of tumor margins and understanding of the relationships with neighboring structures (6, 21). ioUS B-mode, however, is limited to recognizing only the larger vessels, and it does not give any information concerning flow in the lesion's vascular tree (15, 20).

Power Doppler imaging allows one to study small and low flow vessels, without the limitation of angle of insonation, but it does not permit one to evaluate blood flow direction and entity. On the other hand, it has a poor temporal resolution, making it difficult to follow the vessels along their course (24). Moreover, it tends to overestimate the small vessels' dimension for blooming artifacts that scatter color signals outside the vessel margins (15, 20).

Color Doppler flow imaging is mainly indicated to estimate the flow entity and direction in a medium or large vessel. This technique is limited by the angle of insonation dependency; therefore, it does not allow one to follow the entire course of a vessel, especially if it is irregularly stretched by a tumor of the SB region (24).

In most of our cases, with color Doppler, we were able to identify and study the flow of major arteries and their divisions that were feeding the tumor or engulfed within the tumor, and for the continuous comparison with preoperative MRI. One practical problem with this technique concerns highly vascularized tumors, such as meningiomas. In meningiomas, color Doppler yields an unclear image that is difficult to interpret, mainly because color Doppler flow images demonstrate low spatial resolution and are prone to artifacts (24).

All these technical problems are encompassed using CEUS, which, as explained previously, is able to show large, small, high-flow, and low-flow vessels simultaneously within a tomographic real-time image. CEUS allows one to follow the vessels along their entire course and to visualize feeding arteries and draining veins (15-17).

The CEUS technique is also capable of highlighting the tumor extension and the residual mass during excision. Furthermore, CEUS provides information regarding lesion perfusion, thus facilitating the surgical strategy. It can also be performed after tumor resection to evaluate vessels integrity after prolonged manipulation (2, 4, 5, 7, 11, 17).

Having been aware that each of the discussed image-guidance solutions is insufficient if used alone, we developed the N-ASG. This approach combines all the positive capacities of individual solutions and overrides the limitations of each solution individually.

The navigation overcomes the major drawback of ioUS, which is imaging understanding and orientation (**Figure 1**). Thanks to the continuous comparison with preoperative imaging, it is always possible to know the spatial orientation of the ioUS image and to identify the structures. In addition, ioUS allows one to correct the loss of accuracy of the NN caused by brain shift and brain distortion (14).

ASG has an incredible spatial resolution, permitting identification of the vessels' position, orientation, flow entity, and relationships within the lesion. The information obtained with ASG is completed by color Doppler and neuronavigation (**Figures 1–3**). The former evaluates blood flow better than ASG alone does. The latter facilitates the understanding of the orientation of ASG images and the naming of the visualized vessel.

In our series, despite the limited number of cases, we were able to highlight the vessels in all cases and to locate them correctly within the surgical field (**Table 1**). Dissection had been performed with navigated ioUS and ASG guidance. Furthermore, it permitted the visualization of tumor vascularization. In tumors such as meningioma, the vascular feeders usually enter from some peduncle and terminate in a tuft of tiny vessels that during resection could cause abundant bleeding (**Figure 3**). The early identification and interruption of feeding arteries lead to a significant reduction of the bleeding.

After tumor debulking, N-ASG was repeated to visualize deep vessels further. Ultrasound contrast agents can be repeated several times during surgery without adverse events.

All major vessels were identified, and we did not experience any vascular damage; however, this multimodal approach is not free from pitfalls. N-ASG, being an US technique, is highly operator dependent.

There is a need for training in ioUS, to become acquainted with unusual tomographic planes and machine settings. Fusion imaging provides a continuous comparison between ioUS and preoperative MRI and facilitates the understanding of the former imaging. Nevertheless, the need to integrate new datasets of information definitely augments the complexity of the procedure.

A specific training regarding the use of US contrast agents is demanded (8, 12). The use of ioUS in SB surgery has also been limited because of the intrinsic difficulty associated with reaching the surgical field. Because of the usually small access points, the mobility of the probe through the craniotomy (because of the presence of the surrounding skull) is limited, with consequent poor and unusual insonation angles. We generally use a probe that measures only 3.5 × 1 cm. It does not require a large bone flap, and it can fit a small pterional craniotomy. Indeed, in this case it is difficult to perform the evaluation on both axis and extreme tilting (that is, however, not required). However, we generally perform a transdural insonation with our linear probe for CEUS visualization, instead of using a small probe to be inserted along the surgical corridor. We do this for two main reasons: the transdural insonation allows a panoramic view of the surgical field, and the resolution is directly related to the size of the probe. An additional pivotal limitation is the presence of calcifications and hemostatic materials, which are highly reflective interfaces and can limit the depth of the field of view.

CONCLUSIONS

The possibility to perform and repeat an angiography several times during SB tumor removal gives a better understanding of the situation, which enables direct visualization and dissection of the vessels during the approach. It also allows the visualization of tumor vascularization and the identification and interruption of feeding arteries, possibly leading to reduced blood loss. After tumor debulking, N-ASG might be repeated to visualize deep vessels further.

We believe that N-ASG might become a new tool in the armamentarium for SB surgery—able to affect the surgical strategy and necessary to reduce the risk of these highly demanding procedures.

REFERENCES

1. Barnes L, Kapadia SB: The biology and pathology of selected skull base tumors. J Neurooncol 20: 213-240, 1994.
2. Engelhardt M, Hansen C, Eyding J, Wilkening W, Brenke C, Krogias C, Scholz M, Harders A, Ermert H, Schmieder K: Feasibility of contrast-enhanced sonography during resection of cerebral tumours: initial results of a prospective study. Ultrasound Med Biol 33:571-575, 2007.
3. Hammoud MA, Ligon BL, el Souki R, Shi WM, Schomer DF, Sawaya R: Use of intraoperative ultrasound for localizing tumors and determining the extent of resection: a comparative study with magnetic resonance imaging. J Neurosurg 84: 737-741, 1996.
4. He W, Jiang XQ, Wang S, Zhang MZ, Zhao JZ, Liu HZ, Ma J, Xiang DY, Wang LS: Intraoperative contrast-enhanced ultrasound for brain tumors. Clin Imaging 32:419-424, 2008.
5. Holscher T, Ozgur B, Singel S, Wilkening WG, Mattrey RF, Sang H: Intraoperative ultrasound using phase inversion harmonic imaging: first experiences. Neurosurgery 60:382-386; discussion 386-387, 2007.
6. Ivanov M, Wilkins S, Poeata I, Brodbelt A: Intraoperative ultrasound in neurosurgery - a practical guide. Br J Neurosurg 24:510-517, 2010.
7. Kanno H, Ozawa Y, Sakata K, Sato H, Tanabe Y, Shimizu N, Yamamoto I: Intraoperative power Doppler ultrasonography with a contrast-enhancing agent for intracranial tumors. J Neurosurg 102:295-301, 2005.
8. Moiyadi A: Objective assessment of intraoperative ultrasound in brain tumors. Acta Neurochirurgica 156:703-704, 2014.
9. Mostbeck G: "Hot topics" in contrast-enhanced ultrasound (CEUS)—introduction. Ultraschall Med 33 (Suppl 1):S1-S2, 2012.
10. Orringer DA, Golby A, Jolesz F: Neuronavigation in the surgical management of brain tumors: current and future trends. Expert Rev Med Devices 9:491-500, 2012.
11. Otsuki H, Nakatani S, Yamasaki M, Kinoshita A, Iwamoto F, Kagawa N: Intraoperative ultrasound arteriography with the "Coded Harmonic Angio" technique. Report of three cases. J Neurosurg 94: 992-995, 2001.
12. Piscaglia F, Nolsoe C, Dietrich CF, Cosgrove DO, Gilja OH, Bachmann Nielsen M, Albrecht T, Barozzi L, Bertolotto M, Catalano O, Claudon M, Clevert DA, Correas JM, D'Onofrio M, Drudi FM, Eyding J, Giovannini M, Hocke M, Ignee A, Jung EM, Klauser AS, Lassau N, Leen E, Mathis G, Saftoiu A, Seidel G, Sidhu PS, ter Haar G, Timmerman D, Weskott HP: The EFSUMB Guidelines and Recommendations on the Clinical Practice of Contrast Enhanced Ultrasound (CEUS): update 2011 on non-hepatic applications. Ultraschall Med 33:33-59, 2012.
13. Pomeranz S, Umansky F, Elidan J, Ashkenazi E, Valarezo A, Shalit M: Giant cranial base tumours. Acta Neurochirurgica 129:121-126, 1994.
14. Prada F, Del Bene M, Mattei L, Lodigiani L, DeBeni S, Kolev V, Vetrano I, Solbiati L, Sakas G, DiMeco F: Preoperative magnetic resonance and intraoperative ultrasound fusion imaging for real-time neuronavigation in brain tumor surgery. Ultraschall Med 36:174-186, 2014.
15. Prada F, Del Bene M, Moiraghi A, Casali C, Legnani FG, Saladino A, Perin A, Vetrano IG, Mattei L, Richetta C, Saini M, DiMeco F: From grey scale B-mode to elastosonography: multimodal ultrasound imaging in meningioma surgery—pictorial essay and literature review. Biomed Res Int 2015:925729, 2015.
16. Prada F, Mattei L, Del Bene M, Aiani L, Saini M, Casali C, Filippini A, Legnani FG, Perin A, Saladino A, Vetrano IG, Solbiati L, Martegani A, DiMeco F: Intraoperative cerebral glioma characterization with contrast enhanced ultrasound. Biomed Res Int 9:2014, 2014.
17. Prada F, Perin A, Martegani A, Aiani L, Solbiati L, Lamperti M, Casali C, Legnani F, Mattei L, Saladino A, Saini M, DiMeco F: Intraoperative contrast-enhanced ultrasound for brain tumor surgery. Neurosurgery 74:542-552; discussion 552, 2014.
18. Rohde V, Spangenberg P, Mayfrank L, Reinges M, Gilsbach JM, Coenen VA: Advanced neuronavigation in skull base tumors and vascular lesions. Minim Invasive Neurosurg 48:13-18, 2005.
19. Rygh OM, Nagelhus Hernes TA, Lindseth F, Selbekk T, Brostrup Muller T, Unsgaard G: Intraoperative navigated 3-dimensional ultrasound angiography in tumor surgery. Surg Neurol 66: 581-592; discussion 592, 2006.
20. Solheim O, Selbekk T, Lindseth F, Unsgard G: Navigated resection of giant intracranial meningiomas based on intraoperative 3D ultrasound. Acta Neurochir (Wien) 151:1143-1151, 2009.
21. Sosna J, Barth MM, Kruskal JB, Kane RA: Intraoperative sonography for neurosurgery. J Ultrasound Med 24:1671-1682, 2005.
22. Tang H, Sun H, Xie L, Tang Q, Gong Y, Mao Y, Xie Q, Zheng M, Wang D, Zhu H, Zhu J, Feng X, Yao Z, Chen X, Zhou L: Intraoperative ultrasound assistance in resection of intracranial meningiomas. Chin J Cancer Res 25:339-345, 2013.
23. Unsgaard G, Gronningsaeter A, Ommedal S, Nagelhus Hernes TA: Brain operations guided by real-time two-dimensional ultrasound: new possibilities as a result of improved image quality. Neurosurgery 51:402-411; discussion 411-412, 2002.
24. Vivien Gibbs DC: Antonio Sassano: Ultrasound physics and technology. Edinburgh: Churchill Livingstone—Elsevier; 2009.

Conflict of interest statement: The research leading to these results has received funding from the European Union Seventh Framework Programme FP7/2007–2013 under grant agreement no. 602923.

Received 19 March 2015; accepted 7 July 2015

Citation: World Neurosurg. (2015) 84, 6:1699-1707.
http://dx.doi.org/10.1016/j.wneu.2015.07.025

*Journal homepage: **www.WORLDNEUROSURGERY.org***

*Available online: **www.sciencedirect.com***

1878-8750/$ - see front matter